LA-UR- 08-5398

*Approved for public release;*
*distribution is unlimited.*

*Title:* Quantum dynamics of the O + OH -> H + O_2 reaction at low temperatures

*Author(s):* Brian K. Kendrick, Goulven Quemener, and Naduvalath Balakrishnan

*Intended for:* Communication in the Journal of Chemical Physics

Los Alamos
NATIONAL LABORATORY
EST. 1943

# Quantum dynamics of the O + OH → H + $O_2$ reaction at low temperatures

Goulven Quéméner, Naduvalath Balakrishnan
*Department of Chemistry, University of Nevada Las Vegas,*
*Las Vegas, NV 89154, United States of America*

Brian K. Kendrick
*Theoretical Division, Los Alamos National Laboratory,*
*Los Alamos, NM-87545, United States of America*

(Dated: August 14, 2008)

We report quantum dynamics calculations of rate coefficients for the O + OH → H + $O_2$ reaction on two potential energy surfaces (PESs) using a time-independent quantum formalism based on hyperspherical coordinates. Our calculations show that the rate coefficient remains largely constant in the temperature range 10 – 39 K, in agreement with the conclusions of a recent experimental study [Carty et al., J. Phys. Chem. A **110**, 3101 (2006)]. This is in contrast with the quantum calculations of Xu et al. [J. Chem. Phys. **127**, 024304 (2007)] which, using the same PES, predicted two orders of magnitude drop in the rate coefficient value from 39 K to 10 K. Implications of our findings to oxygen chemistry in the interstellar medium are discussed.

PACS numbers:

The reaction

$$O(^3P) + OH(^2\Pi) \rightarrow H(^2S) + O_2(^3\Sigma_g^-)$$

is of considerable importance in atmospheric, combustion and interstellar chemistry. In the upper stratosphere and lower mesosphere, it plays a major role in partitioning the relative abundance of OH and $HO_2$ molecules [1–3]. The reaction also plays a key role in the night-time airglow emissions from the hydroxyl radical which has also been recently detected in the atmosphere of Venus [4]. It has been identified as a key reaction in interstellar oxygen chemistry [5–7] and it is considered to be the most important source of oxygen molecules in cold interstellar clouds [8, 9]. As a consequence, the $HO_2$ system has been the topic of numerous electronic structure calculations of its potential energy surface [10–15] as well as dynamics calculations to evaluate its temperature dependent rate coefficients [13, 14, 16–25]. The reaction has also been the focus of a large number of experimental measurements [26–35]. However, there still remains significant discrepancy between measured and computed values of its rate coefficients for temperatures below 200 K, which is the most important region for astrophysical and upper atmospheric applications.

Recently, Carty et al. [35] reported an experimental measurement of rate coefficients for the reaction in the temperature range 39 K to 142 K and observed no variation in the rate coefficients with temperature in this regime. Based on their findings they concluded that the rate coefficient would largely remain constant between 39 to 10 K, temperatures typical of cold interstellar clouds. In contrast to the experimental results of Carty et al. in a recent theoretical work using quantum scattering calculations within the $J$-shifting approximation, Xu et al. [24] reported rate coefficients that precipitously dropped by about two orders of magnitude between 39 K and 10 K. In a subsequent study on oxygen chemistry in the interstellar medium Quan et al. [36] adopted these rate coefficients and showed that the low abundance of molecular oxygen in cold interstellar molecular clouds could be attributed to the small values of the rate coefficients for the O + OH reaction at temperatures below 39 K.

In this Letter we show that the low temperature rate coefficient of the O + OH reaction is very sensitive to the dense resonance structure in the energy dependence of its reaction probability. Furthermore, to accurately calculate the rate coefficient at 10 K, one needs to include reaction probabilities at energies as low as 1 mK. By using a very fine energy grid to compute the reaction probabilities and including results in the cold regime ($T < 1$ K) we obtain nearly temperature independent values of the reaction rate coefficients in the range 10 to 39 K. Our results do merge with those of Xu et al. at temperatures above 300 K where the very low energy regime does not make a significant contribution. We believe that the rate coefficient reported here would provide a more accurate value for modeling oxygen chemistry in the interstellar medium.

The calculations have been performed using the adiabatically adjusting principle-axis hyperspherical (APH) approach of Pack and Parker [37]. In the present work, we employed the ground electonic state ($1\ ^2A''$) of two PESs. We used the XXZLG PES calculated by Xu, Xie, Zhang, Lin, and Guo [14, 15] which was also employed in the study of Xu et al. [24]. For the other surface, we used the diatomics-in-molecule (DIM) PES developed by Kendrick and Pack [12], hereafter referred to as the DIMKP PES. For each value of the total angular momentum quantum number, $J$, and each value of the hyperspherical radius, $\rho$, the wavefunction is expanded onto a basis set of adiabatic functions, which are eigenfunctions of a triatomic hyperangular Hamiltonian. The hyperangular Hamiltonian is diagonalized using an Implicitly Restarted Lanzcos algorithm and a hybrid DVR/FBR primitive basis set [38]. The time-independent Schrödinger equation yields a set of differential close-coupling equations in $\rho$, which is solved using the log-derivative matrix propagation method of Johnson [39]. The log-derivative matrix is propagated to a matching distance where asymptotic boundary conditions are applied to evaluate the reactance matrix $K$ and the scattering matrix $S$. The square elements of the $S$ matrix provide the state-to-state transition probabilities, $P$. The matching distance and all other parameters employed in the calculations are determined by optimization and extensive convergence studies.

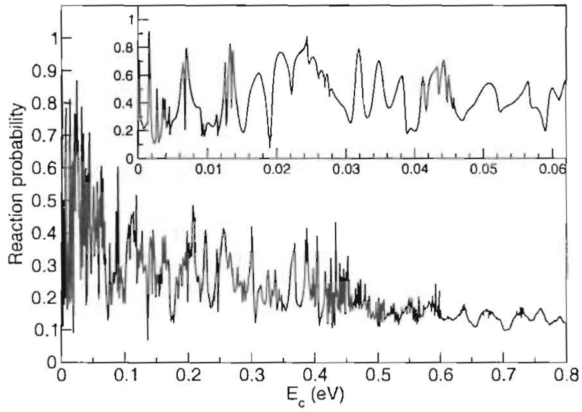

FIG. 1: $J = 0$ reaction probabilities of O + OH($v = 0, j = 0$) $\rightarrow$ H + $O_2$ reaction on the XXZLG PES.

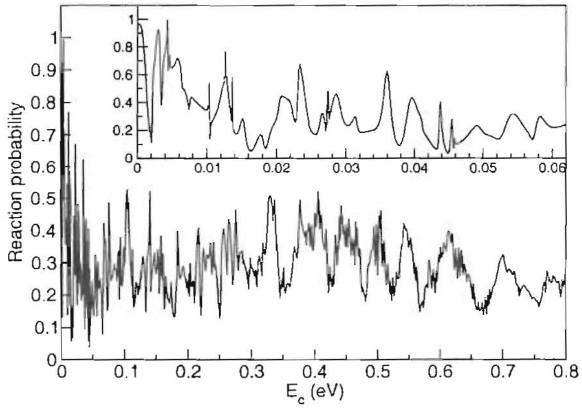

FIG. 2: $J = 0$ reaction probabilities of O + OH($v = 0, j = 0$) $\rightarrow$ H + $O_2$ reaction on the DIMKP PES.

In Fig. 1 we show the $J = 0$ reaction probabilities as a function of the collision energy $E_c$ computed using the XXZLG PES. Corresponding results obtained using the DIMKP PES are shown in Fig. 2. In both figures, the inset shows results for $E_c \leq 0.06$ eV to illustrate the energy resolution required for resolving the resonance features in the reaction probability. Our calculations include reaction probabilities in the energy range $E_c = [10^{-7} - 0.8]$ eV. In the energy range $E_c = [10^{-7} - 10^{-3}]$ eV where no resonance features are present we included 40 energies in a logarithmic scale. Above 0.001 eV, we used the following energy grids: $E_c = [0.0001 - 0.0600; 0.0001]$ eV and $E_c = [0.060 - 0.800; 0.001]$ eV using linear intervals where the last number in the brackets indicates the energy spacing. The reaction probabilities obtained using the two PESs are not identical and they illustrate the sensitivity of results to details of the interaction potential. The global mean is of about 0.3 for the DIMKP PES while it is about 0.2 for the XXZLG PES. The overall trend of the reaction probabilities for the XXZLG PES is a decrease with increase in the collision energy while it oscillates around a value of about 0.3 for the DIMKP PES. The large number of resonances seen in the reaction probabilities comes from quasi-bound states of the $HO_2$ complex.

Accurate determination of the rate coefficients would require calculations of the reaction probabilities for all contributing values of $J$. Computational expense escalates quickly with $J$ unless some angular momentum decoupling approximations are used. Like Xu et al., we use the $J$-shifting approximation [40] to compute the initial state-selected rate coefficients for the reaction. Within the $J$-shifting approximation, the rate coefficient is given by the expression:

$$k_{v,j}(T) = \frac{1}{2\pi\hbar Q_{\rm R}} \times \left( \sum_J (2J+1) e^{-E^J_{\rm shift}/(k_B T)} \right) \times \int_0^\infty P^{r,J=0}_{v,j}(E_c)\, e^{-E_c/(k_B T)}\, dE_c \quad (1)$$

where $k_B$ is the Boltzmann constant and

$$E^J_{\rm shift} = \frac{\hbar^2 J(J+1)}{2\mu(R_{\rm O\text{-}OH})^2} + V^{\rm min}(R_{\rm O\text{-}OH}) \quad (2)$$

is the height of the effective barrier for a given partial wave $J$ in the entrance channel. The quantity $V^{\rm min}(R_{\rm O\text{-}OH})$ is the minimum energy path of the PES as a function of $R_{\rm O\text{-}OH}$ and $Q_{\rm R} = Q_{\rm trans} \times Q_{\rm el}$ is the reactant partition function. For the translational partition function we used the standard formula, $Q_{\rm trans} = \left(\frac{\mu k_B T}{2\pi\hbar^2}\right)^{3/2}$ where $\mu$ is the O−OH reduced mass. For the electronic partition function we used the expression given by Graff and Wagner [18]:

$$Q_{\rm el} = (5 + 3e^{-228/T} + e^{-326/T})(1 + e^{-205/T}).$$

The above expression for the rate coefficient is identical to that used by Xu et al.

The rate coefficients for the $v = 0, j = 0$ initial state obtained using the XXZLG and the DIMKP PESs are shown in Fig. 3 as functions of the temperature along with experimental data from several groups [28, 31, 35] as well as the recommended values by NASA [41] and

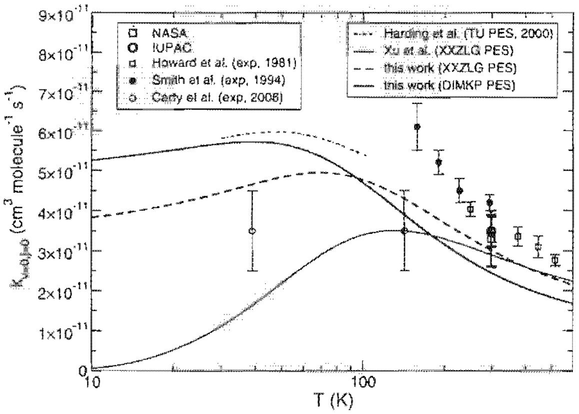

FIG. 3: Rate coefficient of $O + OH(v = 0, j = 0) \rightarrow H + O_2$ as functions of the temperature.

IUPAC [42]. The theoretical results of Xu et al. [24] obtained using the XXZLG PES and the results of Harding et al. [23] obtained using the PES of Troe and Ushakov [13] are also included for comparison. In table I we provide a comparison of our results with the work of Xu et al. and Quan et al. [36] at selected temperatures where experimental results are available.

Both Fig. 3 and table I show that the computed rate coefficients are smaller than the experimental results for temperatures above 200 K. This may be the result of the $J$-shifting approximation. Overall the XXZLG PES provides results in better agreement with the experiments than the DIMKP PES. At $T$=298 K, the rate coefficient calculated using the XXZLG PES is $3.01 \times 10^{-11}$ cm$^3$ molecule$^{-1}$ s$^{-1}$ compared to $2.45 \times 10^{-11}$ cm$^3$ molecule$^{-1}$ s$^{-1}$ obtained using the DIMKP PES. The result on the XXZLG PES is within the reported error bars of the NASA panel recommended value of $3.3 \pm 0.7 \times 10^{-11}$ cm$^3$ molecule$^{-1}$ s$^{-1}$ at 298 K. The computed results on the DIMKP and XXZLG PESs lie within the quoted error bars of Carty et al. at $T$=142 K. While the experimental result of Carty et al. do not show a strong temperature dependence between 142 K and 39 K, the computed results show an increase in the rate coefficient as the temperature is reduced from 142 K to 39 K. The increase is only marginal for the XXZLG PES.

Overall, the temperature dependence of the rate coefficients predicted by the two PESs is very similar. They predict rate coefficients within about 20% for temperatures above 100 K. Between 10 K and 100 K the difference is about 30%. The difference can be explained by the energy dependence of the reaction probabilities shown in the inset of Fig. 1 and Fig. 2. The reaction probabilities are somewhat higher for the DIMKP PES than for the XXZLG PES between 0 – 0.01 eV ($\approx$ 0 – 100 K), leading to an increase in the third multiplicative term in Eq. (1). This can also be explained by the topology of the PESs. The minimum energy path, $V^{\min}(R_{O\text{-}OH})$, of the DIMKP PES features a small "reef" at $R_{O\text{-}OH} = 5.0\ a_0$ whereas it is located at $R_{O\text{-}OH} = 5.4\ a_0$ for the XXZLG PES. For the latter PES the reef is about 0.08 eV higher than that of the DIMKP PES. The location and height of the reef is sensitive to the electronic structure method employed. For certain values of $J$, it becomes an effective barrier. The smaller reef for the DIMKP PES leads to smaller effective barriers especially for higher $J$ values. This enhances the second multiplicative term in Eq. (1) and leads to a higher rate coefficients for the DIMKP PES. For $T$ >100 K, the rate coefficient on the DIMKP PES is smaller than that of the XXZLG PES. At these temperatures the repulsive centrifugal term (first term in Eq. 2) is larger than the height of the PES reef so that it does not play a significant role in the dynamics. Furthermore, as seen in the inset of Fig. 1 and Fig. 2, for collision energies higher than 0.01 eV ($\approx$ 100 K), the DIMKP PES predicts smaller reaction probabilities compared to the XXZLG PES.

| reference | 10 K | 39 K | 142 K | 298 K |
|---|---|---|---|---|
| DIMKP, this work | 5.25 | 5.71 | 3.90 | 2.45 |
| XXZLG, this work | 3.84 | 4.66 | 4.30 | 3.01 |
| Xu et al. [24] | 0.0541 | | | |
| Quan et al. [36] | 0.784 | | | |
| Carty et al. [35] | | 3.5±1.0 | 3.5±1.0 | |
| Lewis et al. [26] | | | | 3.8±0.9 |
| Howard et al. [27] | | | | 3.1±0.8 |
| Robertson et al. [34] | | | | 3.26±0.60 |
| NASA [41] | | | | 3.3±0.7 |
| IUPAC [42] | | | | 3.5±0.4 |

TABLE I: Rate coefficient of $O + OH \rightarrow H + O_2$ given in $10^{-11}$ cm$^3$ molecule$^{-1}$ s$^{-1}$ for different temperatures.

Calculation of rate coefficients involves integration of the Boltzmann distribution of the collision velocities weighted by the reaction probability. The integration has to be performed carefully at low temperatures where the Boltzmann distribution can extend to very low energies. This is especially important for capture-type reactions as the present system for which the rate coefficient does not approach zero as the energy is decreased. The typical temperature in the cold interstellar clouds is about 10 K. At this temperature, one needs to include incident energies as low as $10^{-7}$ eV ($\approx$ 1 mK) in accurately calculating the rate coefficients. We have paid careful attention to include the low energy tail and to use a fine mesh of energies to describe the rich resonance structures in the energy dependence of the reaction probability. As Fig. 3 illustrates, our computed rate coefficients do not show a significant decrease between 142 K and 39 K, consistent with the experimental results of Carty et al. Though no experimental data are available for temperatures below 39 K, our results on both PESs do not predict a dramatic decrease between 39 K and 10 K. At 10 K we obtain a rate coefficient of $3.84\times10^{-11}$ cm$^3$ molecule$^{-1}$ s$^{-1}$ on the XXZLG PES and $5.25\times10^{-11}$ cm$^3$ molecule$^{-1}$ s$^{-1}$ on the DIMKP PES. Our results are about two orders of magnitude larger than the value of $5.4\times10^{-13}$ cm$^3$ molecule$^{-1}$ s$^{-1}$ reported by Xu et al. [24] using the XXZLG PES. Based on our results, we believe that the use of the rate coefficient calculated by Xu et al. in astrophysical modeling may significantly underestimate the importance of the O + OH reaction as a source of molecular oxygen. While an accurate calculation of the rate coefficient would require the inclusion of many higher angular momentum quantum numbers and non-adiabatic couplings, the present calculations show that special attention must be given in the calculation of low temperature rate coefficients for capture reactions.

In conclusion, we have performed quantum dynamics of the O + OH → H + $O_2$ reaction over a wide range of collision energies on two recent PESs using a time-independent quantum formalism based on hyperspherical coordinates. The computed rate coefficients are in reasonable agreement with experimental measurements and existing recommended values, despite using a $J$-shifting approximation for the evaluation of the rate coefficients. Overall, results on the XXZLG PES are in better agreement with the experimental results compared to the DIMKP PES. For both PESs, the rate coefficients decrease only slightly as the temperature is decreased from 39 K to 10 K, in agreement with predictions of the latest experimental study. Based on the present results we believe that a re-evaluation of the importance of the O + OH reaction on $O_2$ abundance would be required for describing oxygen chemistry in the interstellar medium.

This work was supported by NSF grants #PHY-0555565 (NB) and #ATM-0635715 (NB). B.K.K. acknowledges that part of this work was done under the auspices of the US Department of Energy at Los Alamos National Laboratory. Los Alamos National Laboratory is operated by Los Alamos National Security, LLC, for the National Nuclear Security Administration of the US Department of Energy under contract DE-AC52-06NA25396. We thank C. Xu, D. Xie, D. H. Zhang, S. Y. Lin, and H. Guo for providing us their PES.

---

[1] D. C. Clary, Mol. Phys. **53**, 3 (1984).
[2] M. E. Summers et al., Science **277**, 1967 (1997).
[3] Y. P. Lee and C. J. Howard, J. Chem. Phys. **77**, 756 (1982).
[4] G. Piccioni et al., A & A **483**, L29 (2008).
[5] A. Dalgarno and J. H. Black, Rep. Prog. Phys. **39**, 573 (1976).
[6] A. F. Wagner and M. M. Graff, ApJ **317**, 423 (1987).
[7] M. M. Graff and A. Dalgarno, ApJ **317**, 432 (1987).
[8] S. Viti et al., A & A **370**, 557 (2001).
[9] I. W. M. Smith, Chem. Rev. **103**, 4549 (2003).
[10] C. F. Melius and R. J. Blint, J. Chem. Phys. Lett. **64**, 183 (1979).
[11] M. R. Pastrana, L. A. M. Quintales, J. Brandão, and A. J. C. Varandas, J. Phys. Chem. **94**, 8073 (1990).
[12] B. Kendrick and R. T Pack, J. Chem. Phys. **102**, 1994 (1995).
[13] J. Troe and V. G. Ushakov, J. Chem. Phys. **115**, 3621 (2001).
[14] C. Xu, D. Xie, D. H. Zhang, S. Y. Lin, and H. Guo, J. Chem. Phys. **122**, 244305 (2005).
[15] D. Xie et al., J. Chem. Phys. **126**, 074315 (2007).
[16] J. A. Miller, J. Chem. Phys. **84**, 6170 (1986).
[17] J. Davidsson and G. Nyman, Chem. Phys. **125**, 171 (1988).
[18] M. M. Graff and A. F. Wagner, J. Chem. Phys. **92**, 2423 (1990).
[19] A. J. C. Varandas, J. Brandão, and M. R. Pastrana, J. Chem. Phys. **96**, 5137 (1992).
[20] T. C. Germann and W. H. Miller, J. Phys. Chem. A **101**, 6358 (1997).
[21] D. E. Skinner, T. C. Germann, and W. H. Miller, J. Phys. Chem. A **102**, 3828 (1998).
[22] A. Viel, C. Leforestier, and W. H. Miller, J. Chem. Phys. **108**, 3489 (1998).
[23] L. B. Harding, A. I. Mergoiz, J. Troe, and V. G. Ushakov, J. Chem. Phys. **113**, 11019 (2000).
[24] C. Xu, D. Xie, P. Honvault, S. Y. Lin, and H. Guo, J. Chem. Phys. **127**, 024304 (2007).
[25] S. Y. Lin, H. Guo, P. Honvault, C. Xu, and D. Xie, J. Chem. Phys. **128**, 014303 (2008).
[26] R. S. Lewis and R. T. Watson, J. Phys. Chem. **84**, 3495 (1980).
[27] M. J. Howard and I. W. M. Smith, Chem. Phys. Lett. **69**, 40 (1980).
[28] M. J. Howard and I. W. M. Smith, J. Chem. Soc., Faraday Trans. **277**, 997 (1981).
[29] N. Cohen and K. R. Westberg, J. Phys. Chem. Ref. Data **12**, 531 (1983).
[30] K. S. Shin and J. V. Michael, J. Chem. Phys. **95**, 262 (1991).
[31] I. W. M. Smith and D. W. A. Stewart, J. Chem. Soc., Faraday Trans. **90**, 3221 (1994).
[32] D. L. Baulch, et al., J. Phys. Chem. Ref. Data **23**, 847 (1994).
[33] R. Robertson and G. P. Smith, Chem. Phys. Lett. **358**, 157 (2002).
[34] R. Robertson and G. P. Smith, J. Phys. Chem. A **110**, 6673 (2006).
[35] D. Carty, A. Goddard, S. P. K. Kohler, I. R. Sims, and I. W. M. Smith, J. Phys. Chem. A **110**, 3101 (2006).
[36] D. Quan et al., ApJ **681**, 1318 (2008).
[37] R. T Pack and G. A. Parker, J. Chem. Phys. **87**, 3888 (1987).
[38] B. K. Kendrick, R. T Pack, R. B. Walker, and E. F. Hayes, J. Chem. Phys. **110**, 6673 (1999).
[39] B. R. Johnson, J. Comp. Phys. **13**, 445 (1973).
[40] J. M. Bowman, J. Phys. Chem. **95**, 4960 (1991).
[41] S. P. Sander et al., Chemical kinetics and photochemical data for use in atmospheric studies. Evaluation no. 14, Jet Propulsion Laboratory, Pasadena, CA, 2003. Available from: http://jpldataeval.jpl.nasa.gov.
[42] R. Atkinson et al., Atmos. Chem. Phys. **4**, 1461 (2004). Available from: http://www.iupac-kinetic.ch.cam.ac.uk.